



Improving the Tribological and Mechanical Behavior of Recycled Babbitt Alloys Through Zinc Alloying for Sliding Bearing Applications

Muslim Ali^{1*}, Jabbar H. Mohammed², Ameer Ghalib Mortidha³, Ahmed A. Zainulabdeen², Muhanad Hamed Mosa⁴, Saleem Jasim Abbas⁵

¹ Prosthetics and Orthotics Engineering Department, College of Engineering, University of Kerbala, Kerbala 56001, Iraq

² Materials Engineering College, University of Technology- Iraq, Baghdad 10066, Iraq

³ General Directorate of Vocational Education, Ministry of Education, Al-Karkh I, Baghdad 10001, Iraq

⁴ Mechanical Engineering Department, College of Engineering, University of AlQadisiyah, Al-Diwaniyah 58002, Iraq

⁵ Mechanical Power Technical Engineering Department, College of Engineering and Technologies, Al-Mustaqbal University, Babil 51001, Iraq

Corresponding Author Email: muslim.m@uokerbala.edu.iq

Copyright: ©2026 The authors. This article is published by IETA and is licensed under the CC BY 4.0 license (<http://creativecommons.org/licenses/by/4.0/>).

<https://doi.org/10.18280/acsm.500208>

ABSTRACT

Received: 10 February 2026

Revised: 19 April 2026

Accepted: 24 April 2026

Available online: 30 April 2026

Keywords:

recycled Babbitt alloy, zinc addition, microstructure, wear performance, hardness

In this study, the effect of zinc additions (1–4% wt) on the microstructure, hardness, wear resistance, and ductility of recycled tin-based Babbitt alloys was studied. The controlled casting process was used to produce the alloys, which were then characterized and analyzed by X-ray fluorescence (XRF) spectroscopy, optical microscopy, Vickers hardness, pin-on-disc wear (with 20 N load, 2 m/s sliding speed), and compression testing. The results reveal that the incorporation of zinc contributes to high levels of microstructural homogeneity and the refinement of grains, resulting in high ductility and wear resistance. This was despite the zinc addition at 1% wt led to a decrease in hardness, but this was compensated by a significant enhancement of the wear performance. The alloy with 4% Zn showed the most desirable mix of the elements, with good wear resistance (wear rate decrease from $0.85 \pm 0.04 \text{ mm}^3/\text{N}\cdot\text{m}$ to $0.42 \pm 0.03 \text{ mm}^3/\text{N}\cdot\text{m}$) and ductility, with the relative loss of hardness being moderate (decrease from 26–24.7 HV), making it the most preferred of all the tested formulations.

1. INTRODUCTION

Babbitt alloys are a well-known group of alloys (mainly tin (Sn), antimony (Sb) and copper (Cu) that have the best tribological behavior (low friction, high conformability and good load carrying capacity) when subjected to dynamic mechanical and thermal loads. The alloys of Babbitt had been relied on the development of friction layers (mostly tin-rich layers) and mechanical support of hard metal compounds (β -SbSn, γ -Cu₆Sn₅). These systems contribute to low friction and excessive wear resistance. These characteristics make them irreplaceable in some of the most important sliding bearing uses in a variety of fields including automotive engines, turbines, marine engines and industrial machinery [1, 2].

Recycling of the Babbitt alloys has been the center of interest because of the increasing demand in the world to have manufacturing and reusing of materials that are environmental friendly. Savage recycling does not only reduce the environmental impact of mining the raw materials, but also reduces the costs of production and industrial wastes, which is consistent to the contemporary green engineering practices [3, 4]. However, recycled Babbitt alloys are likely to experience mechanical degradation as regards to microstructural heterogeneities as well as impurity accretion during the reprocessing. All of them result in reduced hardness, reduced

ductility and wear resistance that limits their applications in high performance [5, 6]. Alloying has been directed as the most concentrated method of modifying compositions to raise or lower the mechanical properties of Babbitt alloys. Some of the elements that have been extensively investigated on this aspect include Copper, Sb and Pb [7-10]. Despite the fact that, Cu may enhance the corrosion resistance, wear performance, Sb may enhance hardness and mechanical strength, the use of Pb is not an environmental friendly option since it has a toxicological impact on the environment and researchers are making an effort to identify safer options [11].

Zinc (Zn) was considered a potential candidate for this type of alloy. Zinc was used as an additive in this study because it is a more economical, abundant, non-toxic, and environmentally friendly element than lead or bismuth. Furthermore, zinc does not form brittle intermetallic compounds in tin-antimony-copper alloys, is partially soluble in tin, and is used to modify the dimensions and dispersion of SbSn and Cu₆Sn alloys, improving grain shape and corrosion resistance. The use of high zinc additives may result in excessively brittle alloys or exhibit segregation of their components. Simultaneously, this may provide slow growth of the alloys with higher zinc content and the deposition of high-quality SnSb particles at grain boundaries, thereby enhancing corrosion resistance and creep behavior at high temperatures.

Recent findings have also indicated that small zinc additions not only improve microstructure but also form high-quality SnSb particles at grain boundaries, helping to enhance corrosion resistance and creep behavior at high temperatures. Specifically, Zainulabdeen et al. [12] demonstrated improved particle distribution and mechanical stability using zinc-modified tin alloys. The tribological and mechanical improvement of Babbitt alloys for sliding bearing applications have been widely studied in recent years. Zhu et al. [13] discussed the significance of controlling composition of Babbitt alloys, where they reported that ZSnSb11Cu6 and ZSnSb12Cu6Cd1 Babbitt alloys have excellent tribological properties when operating under oil lubricated conditions. In a similar study, Liu et al. [14] studied Babbitt alloys in simulated conditions for wind turbines and found that the wear properties of these alloys are extremely sensitive to the sliding and loading conditions. Wei et al. [15] also pointed out that the mechanical properties and tribological properties of tin-based Babbitt alloys are significantly improved with the refinement of microstructures. Advanced processing routes improved the properties of the surface layers, such as their hardness, and the tribological behavior, as shown by further investigations by Jin et al. [16] that compared the tribological and surface properties of two different types of Babbitt layers: conventionally cast and laser-clad. The importance of microstructure has also been discussed in other studies: Alcover Junior and Pukasiewicz [17] reported that the microstructures of Babbitt coatings prepared by arc-spray method are dendritically refined, which resulted in better wear resistance. Ganiev et al. [18] showed that the addition of zinc affects the thermal behavior of PbSb15Sn10 Babbitt alloys for sliding bearing applications. However, most studies have been limited to primary (non-recycled) alloys or arc deposition environments, and less research has been conducted on recycled Babbitt systems. Thus, the understanding of the effect of zinc addition on the tribological and mechanical properties of recycled Babbitt alloys manufactured using conventional casting processes remains significantly limited. In particular, the combined effects of zinc on phase distribution, wear resistance, hardness degradation, and compressive deformation behavior in systematically recycled systems have not yet been elucidated. This is one of the gaps we will seek to address by investigating the latest technologies.

The objective of the work is to critically assess the impact of zinc addition (1%, 2%, 3%, and 4% by weight) on the microstructure and mechanical characteristics of recycled tin based Babbitt alloys such as hardness, ductility and wear resistance. The given study is likely to result in a structure-property relationship that may be applied to determine the best zinc concentrations to produce high-performance, environmental bearing materials that can be used in the production of complex engineering products.

2. EXPERIMENTAL PART

2.1 Casting process

In this study, a stringent methodology was necessary in castings production because they were relevant in the homogeneity of the distributive of the elements and homogeneity of everything in the properties of the alloys. It has been done in a series of controlled operations to obtain the desirable mechanical and microstructural characteristics of the

zinc-modified recycled Babbitt alloys.

The scrap bearing alloys that were used as raw materials were examined visually to check whether they were dirty, corroded and had traces of foreign materials. This scrap was then treated to mechanical cleaning, acetone-degreased and then preheated at 150 °C for one hour to get rid of any moisture and volatile residues.

The raw materials were prepared, with a standard recycled tin-based Babbitt alloy and elemental zinc. Zinc was introduced in the alloy in weight percentages of 1, 2, 3 and 4 to ascertain how it affected the performance of the alloy. Mechanical cleaning of all materials was done to ensure that any contaminants and oxides on the surface were removed prior to melting to ensure that chances of degrading the final product as a result of impurities.

Electric resistance furnace was used to smelt with a temperature of more than 1000 °C. However, the operating temperature was set at 450 °C so that the tin and alloying material could be melted and the volatilization particularly Zinc was minimized. Once the base alloy was completely melted, it was stirred constantly with the aid of an inert ceramic rod to bring about homogeneity. Zinc was then added in small quantities depending on the recommended percentages of weight. The batches of melted zinc were stirred at 10–15 minutes in the controlled atmosphere to ensure the homogeneity of the zinc added to the batches with the aim of preventing the processes of segregation and the emergence of local concentration gradients.

After homogenization, the molten alloy was carefully poured into preheated steel molds at 250 °C to minimize thermal shock zones, thus preventing internal stresses or cracking due to solidification. The pouring process was carried out at a controlled, layered rate to avoid turbulence and air intrusion, which could lead to porosity and subsurface voids. Solidification occurred during cooling under ambient air conditions, ensuring proper heat dissipation. This preserved the integrity of the microstructure over time and reduced the likelihood of unwanted phase shifts or crack formation.

After solidification and cooling to room temperature, the castings were carefully removed from the molds and subjected to conventional surface preparation, including grinding and polishing. These procedures ensured the samples were adequately prepared for further microscopic and mechanical analyses. Throughout the entire casting process, careful and thorough attention was paid to the main processing parameters, such as melting temperature, stirring time, and proportions of zinc added, with strict adherence to repeatability and prevention of any defect that could negatively affect the final properties of the alloy.

2.2 X-ray fluorescence spectroscopy test

X-ray fluorescence (XRF) spectroscopy was employed to accurately and efficiently determine the elemental composition of the recycled Babbitt alloy specimens. This method is non-destructive, meaning that it does not cause any damage to the sample during analysis (the analysis was repeated three times per sample in current study). The advantage of this technique is that it requires simple sample preparation and allows the chemical elements in the sample to be analyzed at concentrations ranging from parts per million (ppm) to 100%, whether they are major or trace elements.

XRF analysis was performed on Babbitt samples at the Ministry of Science and Technology Planning

Center/Materials Research Department using a wavelength-dispersive X-ray fluorescence spectrometer (WD-XRF), with instrument accuracy of $\pm 0.1\%$.

To minimize contamination, care was taken in the preparation of the alloys by carefully cleaning and conducting controlled melting of the raw materials. The major alloying elements (Sn, Sb, Cu and Zn) were determined using WD-XRF and were found to be stable; no abnormal compositional variations were identified between the samples investigated. In fact, the identified trace elements (impurities) (e.g., Al, Ni, Fe, Bi, Pb) were not quantitatively assessed as they were not present in sufficient quantities for the equipment used, the systematic changes in both the microstructure and properties of the material were strongly correlated with the incremental addition of Zn, with Zn being the main contributor to the observed behaviour. A more detailed impurity assessment is recommended for future work with the use of techniques with higher sensitivity, e.g., inductively coupled plasma optical emission spectrometry (ICP-OES) or scanning electron microscopy with energy dispersive spectroscopy (SEM-EDS).

Table 1 lists the chemical composition of recycled Babbitt alloys, confirming successful zinc incorporation.

Table 1. Chemical composition of recycled Babbitt alloys with zinc additions (wt.%)

| Alloy | Sn (%) | Sb (%) | Cu (%) | Zn (%) |
|----------------|--------|--------|--------|--------|
| Nominal (Base) | 88–90 | 7–8 | 3–4 | 0 |
| Base (Actual) | 88.19 | 7.34 | 3.86 | 0 |
| 1% Zn | 87.22 | 7.29 | 3.82 | 0.97 |
| 2% Zn | 86.28 | 7.25 | 3.79 | 1.98 |
| 3% Zn | 85.33 | 7.21 | 3.77 | 2.96 |
| 4% Zn | 84.39 | 7.17 | 3.74 | 3.95 |

2.3 Sample preparation for microscopic examination

After sample preparation, each sample was cut using a lathe, and then grinding and polishing were carried out using a grinding and polishing machine (Mo Pao 160E). Sandpaper with different grit sizes ranging from 400 to 2000 (according to ASTM standard) was used for grinding. Then the samples were polished using a diamond paste with grit size of 0.25 microns, and then the samples were washed with water and ethanol and dried. To show the microstructure of the samples, an etching agent consisting of (2.5 ml of FeCl_3 , 10 ml of HNO_3 , and 100 ml of H_2O) was used. The samples were immersed in the etching solution for a short period of time (10–15 s) and then washed and dried again. After completing the preparation process, the microstructure of the samples was

examined using a light microscope (Model MTM-1A, BEL-Italy). Magnifications of $20\times$ and $40\times$ were used to examine the microstructural morphology and identify the different phases in the alloy.

2.4 Vickers microhardness test

The hardness of the samples was measured using a Vickers microhardness tester, where the test was performed at a load of 100 grams for 10 seconds holding time (HV0.1) according to ASTM-E384 standard. Hardness measurements were taken at three different areas of the sample: at the edge, midway between the edge and the center, and at the center. Three hardness measurements were performed in each region ($n = 3$), and the results were recorded as mean \pm standard deviation. These tests allowed to determine the distribution of hardness in the sample and the effect of zinc addition on the hardness of the alloy.

2.5 Wear test

The wear test was performed according to strict criteria of the ASTM G99 using a pin-on-disc device in cylindrical specimens made of cast material having a diameter of 10 mm and a height of 25 mm. Fabricated specimens were finished with care before conducting the wear test. Each specimen was vertically fixed to a stainless-steel disk (surface hardness: 60 HRC, surface roughness: 0.15 $\mu\text{m Ra}$, and track radius of 69 mm) with a constant velocity of 2 m/s (277.4 rpm) and dry sliding condition. A normal load 20 N was used, and the tribological assessment was obtained over discrete times of 5, 10, 15 and 20 minutes at ambient temperature (25 $^\circ\text{C}$). The mass loss of the specimen was noted after the post-testing so as to calculate the rate of wear as per Eq. (1).

$$SWR = \frac{\Delta m}{\rho p x} \quad (1)$$

where, Δm is the average mass loss (g), x is the sliding distance (m), p is the applied load (N) and ρ is the material density ($\text{g}\cdot\text{mm}^{-3}$). Total sliding distance x can be calculated as follows:

$$x = 2\pi D n t \quad (2)$$

where, D is the distance from the center of sample to the center of disc in meter, n is the Rotational speed (rpm), and t is the sliding time of running in minute (5,10,15,20 min.).

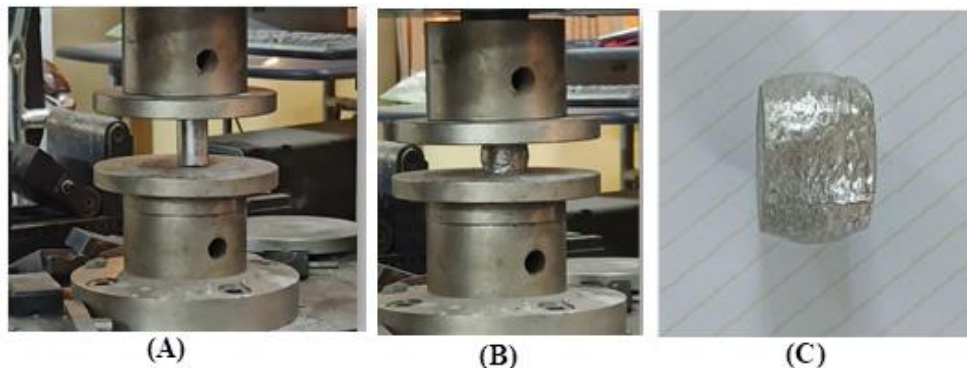


Figure 1. Compression test steps (A) before compression, (B) after compression, (C) compressed sample

2.6 Compressive test

The compression test was performed using a computerized universal testing machine (WDW-50) in the laboratories of the University of Technology- Iraq / Materials Engineering Department. The samples were prepared with standard dimensions according to ASTM E-9 standard and tested in the casting direction (longitudinal orientation). A maximum compressive force of up to 100 kN was applied to the samples, with strain rate of 0.001 s^{-1} , and stress-strain curves were recorded. These tests showed the behavior of the alloy under loading and soft material compression over time. The steps of compressive test are shown in Figure 1.

All mechanical and tribological tests were performed three times ($n = 3$) to ensure the reproducibility and reliability of the experimental results. The values shown are presented as mean \pm standard deviation (SD).

3. RESULTS AND DISCUSSION

3.1 Effect of zinc addition on the microstructure

Optical microscopic analysis observed significant difference in the microstructures of recycled Babbitt alloys following addition of zinc. Based on the characteristic morphology reported in previous studies of Sn based Babbitt alloys the observed phases are believed to be mainly the α -phase (Sn-rich matrix phase), the β -phase (SnSb intermetallic compounds), and the γ -phase (Cu_6Sn_5 intermetallic compounds). In the present work however, SEM-Backscattered Electron (BSE), EDS mapping, and X-ray diffraction (XRD) analysis were not performed so the phase identification should be considered preliminary and morphology-based. As the concentration of Zn increased, the microstructure was progressively refined and the homogeneity of the distribution of the different phases was enhanced, especially at higher concentrations of Zn, which confirms the effect of Zn on grain refinement and microstructural stabilization.

The unmodified alloy (0% Zn) showed the presence of three distinct phases: the α -phase (Sn matrix with dissolved Sb and Cu), β -phase (SbSn intermetallic), and γ -phase (Cu_6Sn_5 with star- or needle-like morphology), as depicted in Figure 2.

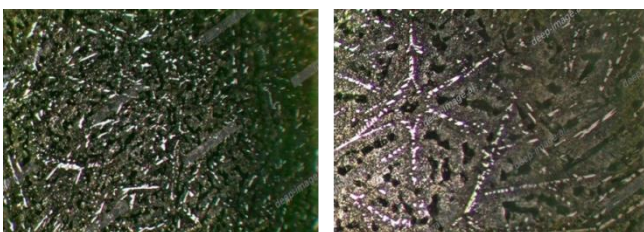


Figure 2. The microstructure of as cast Sn based Babbitt alloy (zoom power 20 \times , and 40 \times)

The introduction of 1 wt% zinc contributed to an increase in the uniformity of phase distribution and a marked improvement in the grain size of the β phase. Grain size estimation using the linear cross-section method (ASTM E112) showed a decrease in the average grain size compared to the base alloy, indicating that zinc acts as a grain modifier (Figure 3). Nonetheless, this enhanced structural homogeneity was accompanied by a reduction of compressive behavior,

which is probably due to a reduced presence of hard interfacial compounds. These observations support previous reports, which highlight the importance of zinc in influencing the grain growth kinetics and promoting the development of a uniform microstructure [19].

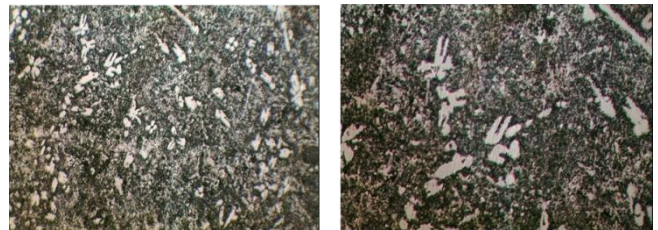


Figure 3. The microstructure of Babbitt alloy with 1 wt. % Zn addition (zoom power 20 \times , and 40 \times)

With a 2 wt.% Zn concentration, the alloy showed higher grain refinement and dispersed distribution of the phase, which is symptomatic of increased nucleation during solidification (Figure 4). Though this caused a minimal increase of hardness it was lower than that which was observed in the base alloy. Ren et al. [6] also reported such effects by showing the refining properties of zinc and its ability to promote the formation of intermetallic phases.

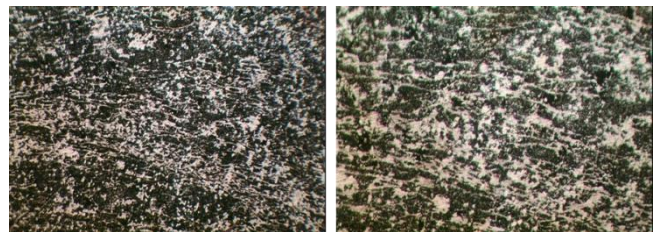


Figure 4. The microstructure of Babbitt alloy with 2 wt.% Zn addition (zoom power 20 \times , and 40 \times)

In the sample with 3% zinc, the microstructure continues to exhibit increased uniformity; however, the corresponding enhancement in hardness becomes less significant (Figure 5). While the addition of zinc at this concentration results in a modest increase in hardness relative to the 2% zinc sample, it still does not reach the hardness level observed in the unalloyed base material.

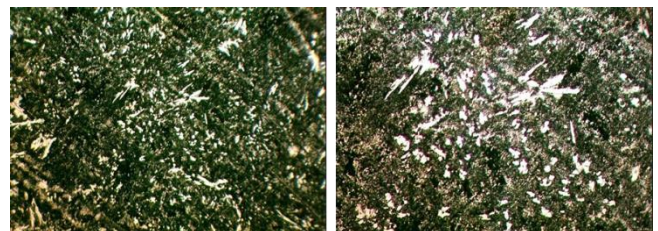


Figure 5. The microstructure of Babbitt alloy with 3 wt. % Zn addition (zoom power 20 \times , and 40 \times)

The microstructure is further refined with finer grains and a more homogeneous distribution of phases at 4% zinc content (Figure 6). This implies that zinc plays a leading role in refining grains, as well as, enhancing the dispersion of phases. However, the alloy fails to reach peak hardness even with the better microstructural characteristics, with the alloy still being weaker than the base alloy. This decrease is probably caused

by the fact that a greater concentration of zinc is more likely to result in increased plasticity that adversely affects hardness.

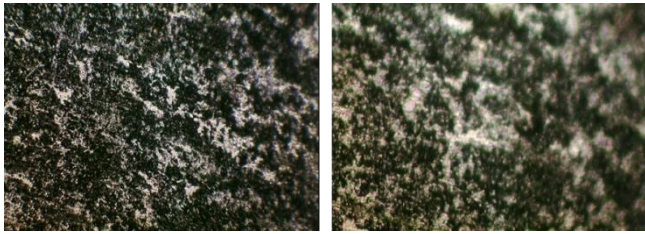


Figure 6. The microstructure of Babbitt alloy with 4 wt. % Zn addition (zoom power 20×, and 40×)

To substantiate these findings, an image fractional analysis of the main intermetallic phases (β and γ) was carried out on standard micrographs at the same magnification level using ImageJ software. It was observed that there was a progressive reduction in the ratio of the coarse interfacial area with the increasing zinc content, especially between 3 and 4 wt. This reduction is the cause of the reduction of hardness observed with the lowering contribution of the solid phases and a finer and more homogeneous distribution of the phases is beneficial in improving the mechanical stability and wear resistance.

3.2 Effect of adding zinc on hardness

As mentioned in the previous section, the results of the hardness test show that adding zinc leads to a general decrease in the hardness of the alloy, as shown in Figure 7. The initial hardness of the pure alloy was 26.0 ± 0.5 HV, but with the addition of 1% zinc, the hardness decreased to 17.5 ± 0.4 HV. This decrease can be explained by the fact that zinc contributes to modifying the internal structure of the alloy so as to reduce the proportion of solid phases such as γ and β , which leads to lower hardness. Furthermore, zinc enhances grain refinement and improves phase dispersion, leading to improved frictional stability, but this results in a more flexible microstructure and, consequently, lower hardness. Additionally, the solid-solution softening effect of zinc in the tin matrix likely contributes to the observed decrease, as zinc atoms disrupt the crystal lattice, reducing dislocation resistance compared to the stiffer structure promoted by copper- and antimony-rich intermetallic phases.

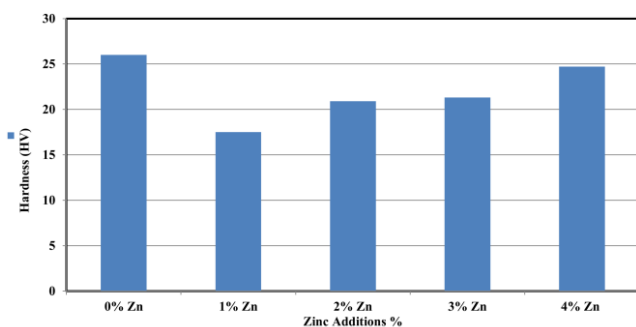


Figure 7. The Vickers hardness of Babbitt alloy with different Zn additions

When the percentage of zinc is increased to 2% and 3%, the hardness increases slightly to 20.9 ± 0.3 HV and 21.3 ± 0.4 HV, respectively, but it remains lower than the original hardness of the pure alloy. This slight improvement in

hardness can be explained as a result of improving the phase distribution and refining of the grains, but these improvements are not sufficient to compensate for the basic negative effect of adding zinc on hardness.

When 4% zinc is added, the hardness increases slightly to 24.7 ± 0.5 HV, but remains lower than that of the pure alloy. This relative increase may be due to the improvement of the homogeneity of the microstructure and the reduction of the grain size, which enhances the alloy's resistance to mechanical deformation. Compared to primary Babbitt alloys, which typically exhibit hardness values around 28–30 HV, recycled alloys containing zinc tend to display reduced hardness levels, restricting their suitability for high-load environments such as heavy-duty turbine systems. However, this drawback may be alleviated by alloying zinc with elements like antimony or copper, which could help balance mechanical performance. Tables 2 and 3 summarize the effect of Zn addition on hardness of Babbitt alloy.

Table 2. Vickers microhardness values (HV0.1) of Babbitt alloys with zinc additions (mean \pm SD, n = 3)

| Alloy | Hardness (HV) |
|--------------|----------------|
| Base (0% Zn) | 26.0 ± 0.5 |
| 1% Zn | 17.5 ± 0.4 |
| 2% Zn | 20.9 ± 0.3 |
| 3% Zn | 21.3 ± 0.4 |
| 4% Zn | 24.7 ± 0.5 |

Table 3. HV0.1 microhardness distribution at different sample locations (mean \pm SD, n = 3)

| Alloy | Hardness (HV) | | |
|--------------|----------------|----------------|----------------|
| | Edge (HV0.1) | Middle (HV0.1) | Center (HV0.1) |
| Base (0% Zn) | 26.4 ± 0.4 | 25.8 ± 0.5 | 25.9 ± 0.6 |
| 1% Zn | 17.8 ± 0.3 | 17.4 ± 0.4 | 17.3 ± 0.5 |
| 2% Zn | 21.2 ± 0.3 | 20.8 ± 0.4 | 20.7 ± 0.3 |
| 3% Zn | 21.5 ± 0.4 | 21.2 ± 0.3 | 21.1 ± 0.5 |
| 4% Zn | 25.0 ± 0.4 | 24.6 ± 0.5 | 24.5 ± 0.4 |

3.3 Effect of zinc addition on wear rate

Wear rate results reveal a pronounced enhancement in the wear resistance of recycled Babbitt alloys with zinc incorporation. The unalloyed base alloy (0% Zn) demonstrated a specific wear rate of 0.85 ± 0.04 mm³/N.m after 20 minutes of sliding at a velocity of 2 m/s under an applied load of 20 N. In comparison, the alloy containing 4 wt.% Zn exhibited a significantly reduced wear rate of 0.42 ± 0.03 mm³/N.m, marking an approximate 50% improvement (as shown in Figure 8 and Table 4).

This enhancement is primarily attributed to the microstructural effects of zinc in improving the phase distribution within the alloy, as zinc improves the homogeneous distribution of hard phases such as SnSb and Cu₆Sn₅ within the tin matrix. This homogeneous distribution reduces the grain size and increases their density, which enhances the wear resistance of the alloy. Moreover, a more uniform grain distribution minimizes the formation of localized stress concentrations, thereby reducing the initiation

and propagation of wear-induced surface damage.

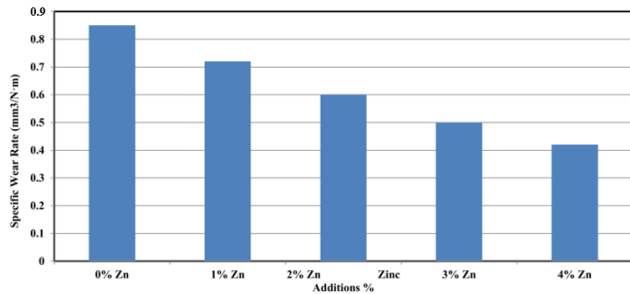


Figure 8. The wear rate of Babbitt alloy with different Zn additions

Table 4. Specific wear rate values of recycled Babbitt alloys after 20 min sliding test (mean ± SD, n = 3)

| Alloy | Specific Wear Rate (mm³/N·m) |
|--------------|------------------------------|
| Base (0% Zn) | 0.85 ± 0.04 |
| 1% Zn | 0.72 ± 0.03 |
| 2% Zn | 0.60 ± 0.03 |
| 3% Zn | 0.50 ± 0.03 |
| 4% Zn | 0.42 ± 0.03 |

The normal wear model, which associates high hardness with better wear resistance does not seem to be the driving force behind the present case, but instead it must be the stability of the microstructure and phase shape as opposed to just the hardness of the base material. This lower wear rate can also be explained by the lower adhesive interactions caused by smoother wear paths and phase boundaries when zinc is greater. According to observed trends, it appears probable that the dominating wear mechanisms at the lower levels of zinc have been involved in adhesion wear and low level of abrasive wear, whereas the more stable, moderate level of abrasive corrosion in higher zinc levels has occurred, even though the material is softer. It was also noted that the wear rate decreases with increase in zinc content when the same loading conditions are used. This could be explained by the fact that the wear process forms a layer of zinc oxide on the surface of the alloy. Although direct surface characterization techniques such as SEM-EDS or X-ray photoelectron spectroscopy (XPS) were not performed in this study, previous studies on zinc-containing bearing alloys have indicated the formation of zinc oxide-rich friction films during dry slip conditions [20]. Thus, this acts as the protective and lubricating layer, and thus there is reduced loss of material due to friction. These were self-lubricating films and in effect, they decreased friction and loss of material during the sliding wear. Interestingly, the sample in which there was 4% of zinc showed the highest percentage of wear rate reduction in comparison with all the rest of the compositions that were tested, thus confirming the hypothesis that a protective layer of zinc oxide develops during wear that protects the alloy against mechanical degradation. It is also suggested that, with increased concentrations of zinc, partial recovery during wear could be promoted and thus prevent the formation of microcracks and further improve wear resistance of the alloy. In addition, the Zn-alloyed recycled system also shows better wear performance as compared to the conventional Sn3Cu Babbitt alloys which usually wear at a rate of about 0.60 mm³/N.m when exposed to similar conditions. These data make zinc an appropriate alloy additive to improve tribology of recycled Babbitt alloys, particularly in

challenging environments such as automobile engine bearings and industrial rotating machinery. As much as the introduction of zinc enhanced wear resistance, there are certain observations that ought to be considered, such as the fact that the zinc can become very high thus reducing hardness as compared to that of the initial unadded alloy. Such reduction in hardness can influence the overall performance of that alloy in some of its applications where the alloy needs to be hard besides possessing wear resistance.

3.4 Effect of zinc addition on compression test

The compression test results are indicated in Figure 9. Depending on the results, it can be seen that alloy 4% zinc exhibited more deformation of 17.5 ± 0.2 mm at 80 MPa which is more than 14.0 ± 0.3 mm of the base alloy which is an indicative of good ductile properties. This will mean that the addition of zinc makes the alloy strong to be under stress without the alloy deteriorating its mechanical properties. This could be explained by the fact that zinc could increase the distribution of the stress in the alloy and reduce local stresses which could lead to mechanical breakdown. The increase in compressive deformation capacity can be attributed to improved grain size and improved phase distribution uniformity, enabling the alloy to deform more uniformly under compressive loading without premature failure. Zn-alloyed recycled Babbitt alloys are more flexible and hence can be used in applications where the bearing loads are dynamic in nature than the Sb-alloyed alloys which typically possess a deformation of approximately 12–15 mm.

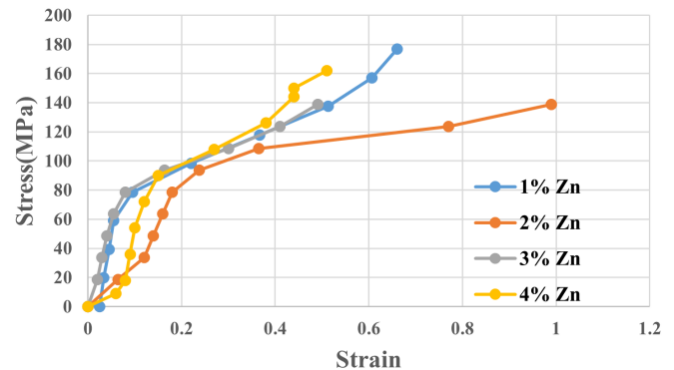


Figure 9. The stress-strain curves of Babbitt alloy with different Zn additions

4. CONCLUSIONS

The impact of zinc addition (0–4 wt%) on the mechanical and tribological behavior of recycled tin-based Babbitt alloys was studied in the current work. The main findings can be summarized as follows:

1. All the percentages of addition of zinc to Babbitt alloys improved wear resistance to a very large extent. The outcomes revealed that the half of the wear ($0.42 \text{ mm}^3/\text{N}\cdot\text{m}$) of the alloy containing 4% zinc exhibited a 50% reduction in wear ($0.42 \text{ mm}^3/\text{N}\cdot\text{m}$) compared to the unalloyed alloy ($0.85 \text{ mm}^3/\text{N}\cdot\text{m}$).
2. The addition of zinc resulted in a decrease in the hardness of the Babbitt alloy (from 26.0 HV to a range of 17.5–24.7 HV), necessitating caution and a balanced approach in applications requiring high surface hardness.

3. Introduction of zinc was accompanied by a little rise in compressive strength but the second effect was on the elongation which declined and showed a trade-off between strength and toughness.

4. Increased zinc content also enhances the alloy's ductility; the 4% Zn alloy achieved a deformation of 17.5 mm, which means that it can be used in a system where dynamic mechanical stress is likely to occur.

5. On the microscopic level, it was found that there was fine grained phase size and distribution between the metals (e.g. Cu₆Sn₅ and SbSn), the homogenous dispersion of zinc is further at 2 wt.

5. LIMITATIONS

1. Future work is recommended to further clarify the role of the residual elements in recycled Babbitt alloys by performing a detailed trace impurity analysis with high-resolution chemical characterization techniques.

2. Further investigations by SEM-EDS and XRD analysis are suggested to confirm phase evolution and identification of any intermetallic compounds containing Zn in the recycled Zn modified Babbitt alloys.

3. To confirm the formation and chemical composition of tribofilms formed during sliding wear, it is recommended to conduct further research using SEM-EDS and XPS surface analysis.

ACKNOWLEDGMENT

The authors are thankful to the Mechanical Engineering Department, College of Engineering, University of Kerbala, Iraq.

REFERENCES

- [1] Cheng, Z., Wang, M., Wang, B., Zhang, L., Zhu, T., Li, N., Zhou, J.F., Jia, F. (2024). Effect of co addition on the microstructure and mechanical properties of Sn-11Sb-6Cu babbitt alloy. *Materials*, 17(22): 5494. <https://doi.org/10.3390/ma17225494>
- [2] Madej, M., Leszczyńska-Madej, B. (2023). Analysis of the effect of the chemical composition of bearing alloys on their wear under wet friction conditions. *Lubricants*, 11(10): 426. <https://doi.org/10.3390/lubricants11100426>
- [3] Ren, X., Chang, Y., Chen, S., Chen, N., Shi, Z., Zhang, Y., Chen, H., Guo, Z., Hu, J., Zhang, G., Xu, H. (2024). Effect of rare earth Y on the microstructure, mechanical properties and friction of Sn-Babbitt alloy. *Coatings*, 14(10): 1325. <https://doi.org/10.3390/coatings14101325>
- [4] Ren, X., Chen, N., Zhang, G., Xu, H., Zhang, Y., Shi, Z., Wang, Z., Liu, Y.J. (2023). Effect of Pb on microstructure and mechanical properties of tin Babbitt alloy. *Journal of Physics Conference Series*, 2478(5): 052007. <http://doi.org/10.1088/1742-6596/2478/5/052007>
- [5] Zhao, J.Y., Sun, K., Liang, G., Xu, C.C., Zhao, J.H., Xue, F., Zhou, J. (2021). Effect of Zn additions on the microstructure and mechanical properties of Sn-Babbitt alloys fabricated by arc deposition. *Journal of Materials Research and Technology*, 15: 6726-6735. <https://doi.org/10.1016/j.jmrt.2021.11.097>
- [6] Ren, X., Chen, H., Chang, Y., Chen, N., Shi, Z., Zhang, Y., Guo, Z., Hu, J. (2024). Effect of Zn on microstructure and wear resistance of Sn-based babbitt alloy. *Crystals*, 14(10): 907. <https://doi.org/10.3390/cryst14100907>
- [7] Runlin, C., Yangyang, W., Qian, J., Jimin, X., Fan, Z., Xiaoyang, Y. (2018). Effect of increasing Cu content on the mechanical properties of tin-based Babbitt. *Rare Metal Materials and Engineering*, 47(6): 1854-1859.
- [8] Leszczyńska-Madej, B., Madej, M., Hrabia-Wiśnios, J. (2019). Effect of chemical composition on the microstructure and tribological properties of Sn-based alloys. *Journal of Materials Engineering and Performance*, 28(7): 4065-4073. <https://doi.org/10.1007/s11665-019-04154-4>
- [9] Alizadeh, R., Mahmudi, R. (2010). Effect of Sb additions on the microstructural stability and mechanical properties of cast Mg-4Zn alloy. *Materials Science and Engineering: A*, 527(20): 5312-5317. <https://doi.org/10.1016/j.msea.2010.05.029>
- [10] Zeren, A., Feyzullahoglu, E., Zeren, M. (2007). A study on tribological behaviour of tin-based bearing material in dry sliding. *Materials & Design*, 28(1): 318-323. <https://doi.org/10.1016/j.matdes.2005.05.016>
- [11] Shi, Z., Xu, H., Zhang, G., Liu, Y., Ren, X. (2023). Effect of Bi content on the microstructure, mechanical and tribological properties of Cu-Sn alloy. *Materials*, 16(20): 6658. <https://doi.org/10.3390/ma16206658>
- [12] Zainulabdeen, A.A., Hashim, F.A., Assi, S.H. (2019). Mechanical properties of tin-based Babbitt alloy using the direct extrusion technique. *IOP Conference Series: Materials Science and Engineering*, 518(3): 032031. <http://doi.org/10.1088/1757-899X/518/3/032031>
- [13] Zhu, L.H., Zhang, W.W., Chang, L., Huang, G.B., Wang, K. (2026). The tribological behavior of ZSnSb11Cu6 Babbitt alloy and ZSnSb12Cu6Cd1 Babbitt alloy under oil lubrication condition. *Journal of Materials Engineering and Performance*, 1-20. <https://doi.org/10.1007/s11665-025-13103-3>
- [14] Liu, W., Wei, L., Zhang, Y., Chen, S., Zhao, G., Gao, G., Wang, H. (2025). Investigation of tribological behavior and failure mechanisms of PEEK-based composites, Babbitt alloy, and CuSn10Pb10 bimetal for wind turbine main shaft sliding bearings under simulated operational conditions. *Tribology International*, 204: 110522. <https://doi.org/10.1016/j.triboint.2025.110522>
- [15] Wei, Z., Shu, H., Qiao, G., Zeng, Q., Wang, G., Jia, Q. (2024). Performance improvement of tin-based Babbitt alloy through control of microstructure. *Alloys*, 4(3): 11. <https://doi.org/10.3390/alloys4030011>
- [16] Jin, J., Ye, J., Xue, H., Xu, Y., Guo, Z., Zhou, Z., Xu, G., Wang, G. (2026). Microstructure and properties of conventional cast versus annular laser-clad babbitt alloy layers for sliding bearings. *Micromachines*, 17(1): 134. <https://doi.org/10.3390/mi17010134>
- [17] Alcover Junior, P.R.C., Pukasiewicz, A.G.M. (2019). Evaluation of microstructure, mechanical and tribological properties of a Babbitt alloy deposited by arc and flame spray processes. *Tribology International*, 131: 148-157. <https://doi.org/10.1016/j.triboint.2018.10.027>
- [18] Ganiev, I.N., Jumaeva, M.B., Khojanazarov, K.M., Odinzoda, H.O., Khudoyberdizoda, S.U. (2025). Influence of zinc on the thermophysical properties and thermodynamic functions of lead Babbitt B

- (PbSb15Sn10). *Journal of Engineering Physics and Thermophysics*, 98(3): 757-763. <https://doi.org/10.1007/s10891-025-03155-6>
- [19] Song, Z.Y., Jin, S.C., Shen, Y.M., Teng, J.B., Lu, B., Zhang, L.C. (2022). Indentation creep behaviors of SnSb8Cu4 Babbitt alloy with Zn and Cu addition. *Mechanics of Materials*, 63(4): 579-585. <https://doi.org/10.2320/matertrans.MT-M2021177>
- [20] Podrabinnik, P., Gershman, I., Mironov, A., Kuznetsova, E., Okunkova, A.A., Grigoriev, S.N. (2023). Study of adaptation processes in tribofilms during friction of antifriction aluminum alloys for journal bearings. *Metals*, 13(12): 1936. <https://doi.org/10.3390/met13121936>